

Smooth relaxed $\text{Si}_{0.75}\text{Ge}_{0.25}$ layers on Si(001) via *in situ* rapid thermal annealing

S. Hong,^{a)} Y. L. Foo,^{b)} K. A. Bratland, T. Spila,^{c)} K. Ohmori, M. R. Sardela, Jr., and J. E. Greene

Materials Science Department and the Frederick Seitz Materials Research Laboratory, University of Illinois, 104 South Goodwin Avenue, Urbana, Illinois 61801

E. Yoon

School of Materials Science and Engineering, Seoul National University, San 56-1, Shilim-dong, Kwanak-ku, Seoul 151-744, Korea

(Received 1 August 2003; accepted 1 October 2003)

Atomically flat, fully strained $\text{Si}_{1-x}\text{Ge}_x$ layers with thicknesses ranging from 8 to 180 nm were grown on Si(001) at 450 °C by gas-source molecular beam epitaxy from $\text{Ge}_2\text{H}_6/\text{Si}_2\text{H}_6$ mixtures. We show that smooth, *relaxed* alloy layers are obtained, without the necessity of using several-microns-thick compositionally graded layers, via *in situ* rapid thermal annealing of fully strained $\text{Si}_{1-x}\text{Ge}_x(001)$ layers at 1000 °C for 10 s. Relaxed $\text{Si}_{0.75}\text{Ge}_{0.25}(001)$ layers with thicknesses of 100–180 nm were found to have surface widths of ≈ 5 nm, comparable to the best results obtained using thick graded buffer layers. © 2003 American Institute of Physics. [DOI: 10.1063/1.1629792]

Obtaining smooth strain-relaxed $\text{Si}_{1-x}\text{Ge}_x$ alloy layers on Si(001) substrates is currently of intense interest due to the possibilities it affords for growing tensile-strained Si overlayers with enhanced carrier mobilities as well as for integration with III–V heterostructures in optical device applications. The conventional method for obtaining relaxed $\text{Si}_{1-x}\text{Ge}_x(001)$ layers is to first grow thick compositionally graded buffer layers, in which the misfit strain is gradually relieved with increasing film thickness, on Si(001).^{1,2} Higher compositional grading rates and/or final Ge concentrations lead to rougher surfaces.² Thus, buffer layer thicknesses of 5–10 μm are typically required in order to obtain relaxed $\text{Si}_{1-x}\text{Ge}_x(001)$ overlayers with root-mean-square surface roughnesses w less than 10 nm. In addition, chemical-mechanical polishing is often used at intermediate stages of graded buffer layer growth in order to reduce the roughness of the final surface.³

A second approach to achieving relaxed alloy layers is postdeposition annealing of $\text{Si}_{1-x}\text{Ge}_x$ films deposited on thin Si(001) layers grown on compliant substrates such as Si-on-insulator (SOI) with SiO_2 as the insulator.^{4,5} The SOI substrates transfer the misfit strain from the alloy layer to the thin Si(001) underlayer as the oxide becomes viscous during high temperature thermal annealing. However, surface roughening values have not been reported.

Spila *et al.*⁶ recently demonstrated the growth of extremely smooth ($w < 0.15$ nm), fully strained $\text{Si}_{0.7}\text{Ge}_{0.3}$ layers on Si(001) by gas-source molecular beam epitaxy (GS-MBE) from hydride precursors at $T_s = 450$ °C. Strain-induced roughening was completely quenched due to the combined effects of the low growth temperature and the cor-

respondingly high steady-state hydrogen coverage $\theta_{\text{H}} = 0.52$ ML resulting in low adatom ascending-step crossing probabilities.

In this letter, we discuss the results of experiments designed to obtain strain-relaxed $\text{Si}_{1-x}\text{Ge}_x(001)$ layers with smooth surfaces without the necessity of growing thick compositionally graded buffer layers or using SOI substrates. We start with flat ($w \leq 0.13$ nm) fully coherent $\text{Si}_{0.75}\text{Ge}_{0.25}(001)$ layers grown by hydride GS-MBE and then relax the alloy films via *in situ* rapid thermal annealing (RTA). The degree of strain relaxation R and the surface width w are determined as a function of layer thickness.

$\text{Si}_{0.75}\text{Ge}_{0.25}(001)$ layers with thicknesses ranging from 8 to 180 nm were grown on Si(001) in a multichamber ultrahigh-vacuum system, with a base pressure of 5×10^{-11} Torr, described in detail in Ref. 7. The system is equipped with *in situ* reflection high-energy electron diffraction (RHEED) and Auger electron spectroscopy (AES). The Si(001) substrates were 1×3 cm², cleaved from 0.5-mm-thick B doped wafers (resistivity = 38–63 Ω cm). Degreasing and substrate cleaning, including wet-chemical oxidation/etch cycles, an UV ozone treatment, UHV degassing, and oxide desorption, are described in Ref. 7. RHEED patterns from substrates subjected to this procedure are 2×1 with sharp Kikuchi lines and no residual C or O is detected by AES. Si(001) buffer layers, 100 nm thick, were deposited at 800 °C prior to growth of the $\text{Si}_{0.75}\text{Ge}_{0.25}(001)$ alloy layers. The latter was carried out at 450 °C using Si_2H_6 and Ge_2H_6 precursor fluxes, delivered through tubular dosers, of 2.2×10^{16} and 1.2×10^{15} cm⁻² s⁻¹, respectively, resulting in a film growth rate of 1.2 nm min⁻¹. Immediately after growth, the samples were subjected to *in situ* RTA; sample heating and cooling rates were 100 °C s⁻¹.

The thickness t and composition x of as-deposited alloy layers were determined by Rutherford backscattering spectrometry carried out with 2 MeV He⁺ ions; the data were analyzed using the RUMP simulation program. High-

^{a)}Present address: School of Materials Science and Engineering, Seoul National University, San 56-1, Shilim-dong, Kwanak-ku, Seoul 151-744, Korea.

^{b)}Present address: Institute of Materials Research and Engineering (IMRE), 3 Research Link, S117602, Singapore.

^{c)}Electronic mail: spila@mrl.uiuc.edu

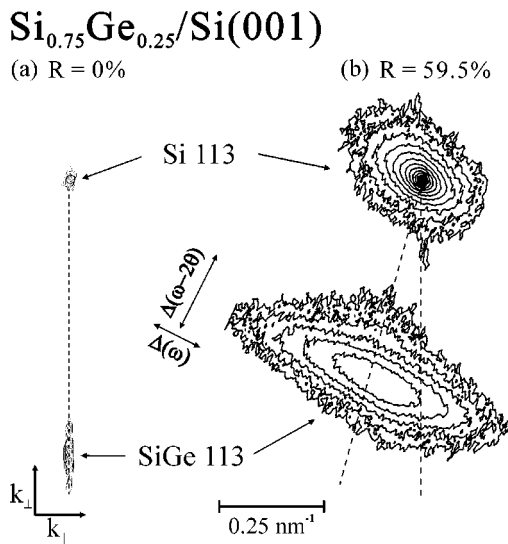


FIG. 1. HR-RLMs around asymmetric 113 Bragg peaks from 180-nm-thick $\text{Si}_{0.75}\text{Ge}_{0.25}$ GS-MBE layers grown at 450°C on Si(001): (a) as-deposited and (b) after *in situ* RTA at 1000°C for 10 s. Peak intensities range logarithmically from 10 to 1.5×10^5 cts s^{-1} .

resolution x-ray diffraction measurements were performed in a Philips X'pert instrument using $\text{Cu } K_{\alpha 1}$ radiation from a double-reflection Ge(220) monochromator with an x-ray mirror which provides an angular divergence of <30 arc sec. The residual strains in both as-deposited and annealed layers were obtained from high-resolution reciprocal lattice maps (HR-RLMs), using a three-reflection Ge analyzer crystal, constructed from successive $\omega-2\theta$ scans at different ω values.

Film morphology and surface roughness were quantified using contact-mode atomic force microscopy (AFM). Height-difference, $G(\rho) = \langle |h_j - h_i|^2 \rangle$, and height-height, $H(\rho) = \langle h_i h_j \rangle$, correlation functions—where h is the height at positions i and j separated by a distance ρ and the brackets correspond to averages over the measured surface—were calculated from the AFM images. Values for the surface width w , which is equivalent to the root-mean-square roughness, are obtained using the relation $2w^2 = G(\rho) + 2H(\rho)$.

Initial RTA experiments showed that while strain relaxation R in annealed layers increases continuously with t , the surface morphology exhibits a transition from strain-induced surface roughening to misfit-dislocation-induced crosshatch patterns at thickness values which depend strongly upon the RTA conditions. We obtain $\text{Si}_{0.75}\text{Ge}_{0.25}(001)$ alloy layers with both a high degree of relaxation and a smooth surface for layers annealed at $T_a = 1000^\circ\text{C}$ for 10 s. Increasing T_a results in a higher R value, but with significantly rougher surfaces. Decreasing T_a yields smoother surfaces but the films remain highly strained.⁸ Thus, we use 10 s, 1000°C RTA in the following experiments.

Typical HR-RLMs around asymmetric 113 reflections from as-deposited and annealed 180-nm-thick $\text{Si}_{0.75}\text{Ge}_{0.25}(001)$ layers are shown in Fig. 1. Diffracted intensities are plotted as iso-intensity contours as a function of the reciprocal lattice vectors k_{\parallel} parallel and k_{\perp} perpendicular to the surface. For the as-deposited layer in Fig. 1(a), the substrate and layer scattering distributions are essentially perfectly aligned in the k_{\parallel} direction showing that the alloy is

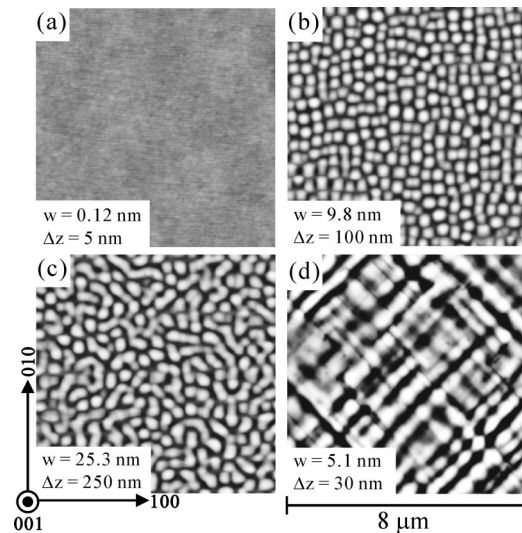


FIG. 2. (a) AFM image of an as-deposited 180-nm-thick GS-MBE $\text{Si}_{0.75}\text{Ge}_{0.25}$ layer grown at 450°C on Si(001). Images of layers grown to thicknesses of (b) 8, (c) 36, and (d) 180 nm and then subjected to *in situ* RTA at 1000°C for 10 s. Δz is the black-to-white grayscale values.

fully commensurate with the substrate. Identical results were obtained for all alloy thicknesses, $t = 8-180$ nm. The layer diffraction contours are nearly symmetric, an indication of high crystalline quality and low mosaicity. Following RTA [Fig. 1(b)], both the substrate and film diffraction peaks exhibit broadening in the ω and k_{\parallel} directions revealing increased surface and/or interface roughness with increased mosaicity. In addition, the position of the layer peak is shifted toward the $\omega-2\theta$ axis, indicative of strain relaxation. k_{\parallel} and k_{\perp} are related to peak positions in $\omega-2\theta$ space through the relationships $k_{\parallel} = 2r_E \sin(\theta) \cos(\omega - \theta)$ and $k_{\perp} = 2r_E \sin(\theta) \sin(\omega - \theta)$ where r_E is the Ewald sphere radius given by $r_E = 1/\lambda$ in which λ is the x-ray wavelength.⁹ For a 113 reflection from an 001-oriented diamond-structure crystal, the in-plane a_{\parallel} and out-of-plane a_{\perp} lattice constants are given by $a_{\parallel} = \sqrt{2}/k_{\parallel}$ and $a_{\perp} = 3/k_{\perp}$.

Measured values of a_{\parallel} and a_{\perp} are used to determine the degree of in-plane layer relaxation $R = (a_{\parallel} - a_s)/(a_0 - a_s)$ where $a_s = 0.543088$ nm is the substrate lattice constant and a_0 is the relaxed alloy lattice parameter. We obtain $a_0 = 0.5485$ nm, in good agreement with measurements from bulk crystals,¹⁰ from the relationship $a_0 = a_{\perp} [1 - 2\nu(a_{\perp} - a_{\parallel})/a_{\perp}(1 + \nu)]$ in which ν is the Poisson ratio. Following *in situ* RTA of the $\text{Si}_{0.75}\text{Ge}_{0.25}(001)$ layer corresponding to Fig. 1(b), $R = 59.5\%$.

An $8 \times 8 \mu\text{m}^2$ AFM image of an as-deposited 180-nm-thick $\text{Si}_{0.75}\text{Ge}_{0.25}(001)$ layer is presented in Fig. 2. As-deposited alloy layers at all thicknesses, $t = 8-180$ nm, are extremely flat with no indication of strain-induced surface roughening. Surface widths w are ≤ 0.13 nm, comparable to that of the Si substrate ($w = 0.09$ nm). For the layer in Fig. 2(a), $w = 0.12$ nm.

Measured w and R values for $\text{Si}_{0.75}\text{Ge}_{0.25}(001)$ layers following *in situ* RTA are plotted as a function of t in Fig. 3. For the thinnest layers ($t \leq 21$ nm), AFM images [e.g., Fig. 2(b)] show that the surface morphology consists of mounds preferentially aligned along $\langle 100 \rangle$ directions. The average in-plane mound separation d for the 8-nm-thick layer in Fig. 2(b) is $d = 10.5$ nm. The surface roughness is

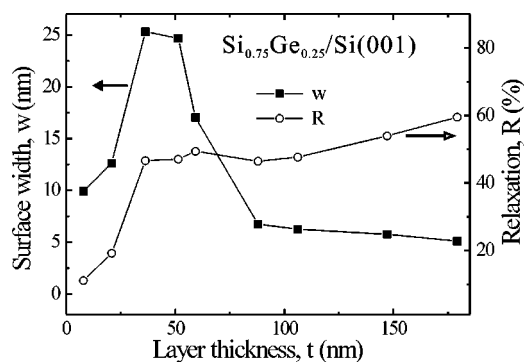


FIG. 3. Surface width w and degree of relaxation R as a function of the thickness t of GS-MBE $\text{Si}_{0.75}\text{Ge}_{0.25}$ layers grown at 450°C on $\text{Si}(001)$ and then subjected to *in situ* RTA at 1000°C for 10 s.

2(b) is $0.2\ \mu\text{m}$. As t is increased to 36 nm, w , d , and R for the annealed layers increase rapidly as the surface mounds coalesce along $\langle 110 \rangle$. For the 36-nm-thick layer [Fig. 2(c)], $w = 25.3\ \text{nm}$ and $R = 50\%$. Further increases in t to $\geq 50\ \text{nm}$ result in a dramatic change in the surface morphology. While w decreases, d continues to increase as the morphology becomes dominated by symmetric ridges aligned, due to the network of misfit dislocations, along orthogonal $\langle 110 \rangle$ directions. Film relaxation $R(t)$ also continues to increase, although much more slowly. Figure 2(d) corresponds to an annealed $t = 180\ \text{nm}$ layer for which $w = 5.1\ \text{nm}$ and $R = 59.5\%$. The in-plane ridge spacing is approximately $0.45\ \mu\text{m}$.

Surface mound formation during the relaxation of strained layers is favorable when the energy increase associated with the larger surface area is overcome by the decrease in the total strain energy of the system.⁶ Preferential mound ordering along $\langle 100 \rangle$ directions is attributed to the anisotropic strain-induced modification of the surface chemical potential. Using numerical finite element calculations for $\text{Si}_{0.75}\text{Ge}_{0.25}$ islands on $\text{Si}(001)$, the strain energy density for a pyramidal island has been shown to have a local maximum near the island edge in the elastically hard $\langle 110 \rangle$ direction while the strain field in the $\langle 100 \rangle$ direction decays monotonically with distance from the island perimeter.¹¹ The local strain energy maximum in $\langle 110 \rangle$ directions gives rise to preferential diffusion toward $\langle 100 \rangle$ island edges during RTA.

AFM results show that our RTA $\text{Si}_{0.75}\text{Ge}_{0.25}(001)$ layers exhibit a surface morphological transition at $t^* \approx 50\ \text{nm}$. At lower thicknesses, film morphology is controlled by strain-induced roughening. However, at $t > t^*$, the layer strain energy is large enough to result in the formation of a sufficiently high dislocation density that the surface morphology becomes dominated by misfit-dislocation-induced roughening. Spila *et al.*¹² have demonstrated that the development of a crosshatch surface structure in compressively strained GS-MBE $\text{Si}_{1-x}\text{Ge}_x(001)$ layers occurs via an interaction between two mechanisms: the formation of multiheight surface steps due to arrays of dislocation pileups on a common glide plane and the growth of self-organized periodic ridges due to uphill mass transport driven by inhomogeneous strain fields around the dislocations. The surface steps enhance uphill adatom migration by acting as preferential H desorption sites.

We attribute the flatness of our relaxed 100–180-nm-thick $\text{Si}_{0.75}\text{Ge}_{0.25}/\text{Si}(001)$ alloy layers to the very rapid, high temperature thermal pulse during RTA together with the large activation energy for dislocation nucleation in $\text{Si}_{1-x}\text{Ge}_x(001)$ which is reported to be $\approx 5\ \text{eV}$ for alloy layers with x between 0.15 and 0.45.¹³ That is, the high strain energy associated with the thicker as-deposited alloy layers combined with the 1000°C RTA pulse are sufficient to allow formation of misfit dislocations, which are much more effective than surface roughening in promoting film relaxation, before the onset of significant mound formation. Hence, misfit dislocations, rather than strain-induced roughening as occurs during post-deposition thermal annealing,^{14,15} dominate the relaxation kinetics during our RTA experiments resulting in the much flatter surfaces that we observe.

In conclusion, we show that, starting with extremely smooth ($w \leq 0.13\ \text{nm}$) fully strained $\text{Si}_{0.75}\text{Ge}_{0.25}$ layers grown on $\text{Si}(001)$ by hydride GS-MBE, smooth relaxed alloy layers can be obtained via *in situ* rapid thermal annealing RTA at 1000°C for 10 s. As the alloy layer thickness is increased, we observe a transition in surface morphology at $t \approx 50\ \text{nm}$. Strain-induced roughening dominates for layers with $t \leq 50\ \text{nm}$, where w and R increase rapidly with t . However, dislocation-induced roughening giving rise to cross-hatch patterns dominates at $t \geq 50\ \text{nm}$. In contrast to strain-induced roughening in thinner layers, w now decreases, while R continues to increase, with increasing film thickness. With 180-nm-thick films, we obtain smooth, relaxed $\text{Si}_{0.75}\text{Ge}_{0.25}$ layers with $w = 5.1\ \text{nm}$ and $R = 59.5\%$.

The authors appreciate the support of the U.S. Department of Energy under Grant No. DEFG02-91ER45439 and use of the Center for Microanalysis of Materials, partially supported by the DOE at the University of Illinois. S.H. and E.Y. were supported by the BK21 program of the Korean Ministry of Education.

¹E. A. Fitzgerald, Y. H. Xie, M. L. Green, D. Brasen, A. R. Kortan, J. Michel, Y. J. Mii, and B. E. Weir, *Appl. Phys. Lett.* **59**, 811 (1991).

²J. W. P. Hsu, E. A. Fitzgerald, Y. H. Xie, P. J. Silverman, and M. J. Cardillo, *Appl. Phys. Lett.* **61**, 1293 (1992).

³M. T. Currie, S. B. Samavedam, T. A. Langdo, C. W. Leitz, and E. A. Fitzgerald, *Appl. Phys. Lett.* **72**, 1718 (1998).

⁴A. R. Powell, S. S. Iyer, and F. K. LeGoues, *Appl. Phys. Lett.* **64**, 1856 (1994).

⁵F. Y. Huang, M. A. Chu, M. O. Tanner, K. L. Wang, G. D. U'Ren, and M. S. Goorsky, *Appl. Phys. Lett.* **76**, 2680 (1999).

⁶T. Spila, P. Desjardins, A. Vailionis, H. Kim, N. Taylor, G. Cahill, J. E. Greene, S. Guillion, and R. A. Masut, *J. Appl. Phys.* **91**, 3579 (2002).

⁷Q. Lu, T. R. Bramblett, N. E. Lee, M. A. Hasan, T. Karasawa, and J. E. Greene, *J. Appl. Phys.* **77**, 3067 (1995).

⁸ R for $t = 150\ \text{nm}$ layers increased from 54% at $T_a = 1000^\circ\text{C}$ to 73.5% at 1100°C , but w also increased from ≈ 5.6 to $12\ \text{nm}$. At $T_a = 800^\circ\text{C}$, w decreased to $\approx 2\ \text{nm}$, but R decreased to 6.1% for the same layer thickness.

⁹P. van der Sluis, *J. Phys. D* **26**, A188 (1993).

¹⁰J. P. Dismukes, L. Ekstrom, and R. J. Paff, *J. Phys. Chem.* **68**, 3021 (1964).

¹¹M. Meixner, E. Schöll, M. Schmidbauer, H. Raidt, and R. Köler, *Phys. Rev. B* **64**, 245307 (2001).

¹²T. Spila, P. Desjardins, J. D'Arcy-Gall, R. D. Twisten, and J. E. Greene, *J. Appl. Phys.* **93**, 1918 (2003).

¹³F. K. LeGoues, P. M. Mooney, and J. Tersoff, *Phys. Rev. Lett.* **71**, 396 (1993).

¹⁴K. M. Chen, D. E. Jesson, S. J. Pennycook, T. Thundat, and R. J. Warrmack, *J. Vac. Sci. Technol. B* **14**, 2199 (1996).

¹⁵C. S. Ozkan, W. D. Nix, and H. Gao, *Appl. Phys. Lett.* **70**, 2247 (1997).